NeuroImage 221 (2020) 117175

Contents lists available at ScienceDirect

NeuroImage

journal homepage: www.elsevier.com/locate/neuroimage

Reduction of somatosensory functional connectivity by transcranial alternating current stimulation at endogenous mu-frequency

Christopher Gundlach[a,b,*], Matthias M. Müller[b], Maike Hoff[a], Patrick Ragert[a,c], Till Nierhaus[a,d], Arno Villringer[a,e,f], Bernhard Sehm[a,f,g,*]

[a] Department of Neurology, Max Planck Institute for Human Cognitive and Brain Sciences, Stephanstraße 1a, 04103 Leipzig, Germany
[b] Department of Psychology, University of Leipzig, 04109 Neumarkt 9-19, Leipzig, Germany
[c] Institute for General Kinesiology and Exercise Sciences, Faculty of Sport Science, University of Leipzig, 04109 Leipzig, Germany
[d] Neurocomputation and Neuroimaging Unit (NNU), Department of Education and Psychology, Freie Universität Berlin, 14195 Berlin, Germany
[e] MindBrainBody Institute at Berlin School of Mind and Brain, Charité Universitätsmedizin Berlin and Humboldt-University, 10099 Berlin, Germany
[f] Department of Cognitive Neurology, University of Leipzig, 04103 Leipzig, Germany
[g] Universitätsklinik Halle (Saale), 06097 Halle (Saale), Germany

ARTICLE INFO

Keywords:
tACS
Mu-alpha
Neural oscillations
fMRI
Somatosensory cortex
Brain stimulation

ABSTRACT

Alpha, the most prominent human brain rhythm, might reflect a mechanism of functional inhibition for gating neural processing. This concept has been derived predominantly from local measures of inhibition, while large-scale network mechanisms to guide information flow are largely unknown. Here, we investigated functional connectivity changes on a whole-brain level by concurrent transcranial alternating current stimulation (tACS) and resting-state functional MRI in humans. We specifically focused on somatosensory alpha-band oscillations by adjusting the tACS frequency to each individual´s somatosensory (mu-) alpha peak frequency (mu-tACS). Potential differences of Eigenvector Centrality of primary somatosensory cortex (S1) as well as on a whole brain level between mu-tACS and sham were analyzed. Our results demonstrate that mu-tACS induces a locally-specific decrease in whole-brain functional connectivity of left S1. An additional exploratory analysis revealed that this effect primarily depends on a decrease in functional connectivity between S1 and a network of regions that are crucially involved in somatosensory processing. Furthermore, the decrease in functional centrality was specific to mu-tACS and was not observed when tACS was applied in the gamma-range in an independent study. Our findings provide evidence that modulated somatosensory (mu-) alpha-activity may affect whole-brain network level activity by decoupling primary sensory areas from other hubs involved in sensory processing.

1. Introduction

Oscillatory activity is a fundamental operational mode across multiple spatiotemporal domains in the central nervous system (Buzsáki and Draguhn, 2004). Alpha-band oscillations (8–12 Hz) are postulated to be involved in guiding information flow across the brain due to an overall inhibitory nature (Foxe and Snyder, 2011; Jensen and Mazaheri, 2010; Klimesch et al., 2007; Palva and Palva, 2007). This functional mode seems to apply to different sensory domains: amplitude fluctuations in the alpha-band are associated with changes in perception of visual stimuli (Ergenoglu et al., 2004; Samaha et al., 2017; van Dijk et al., 2008), auditory stimuli (Strauß et al., 2015; Wöstmann et al., 2016) or somatosensory stimuli (Haegens et al., 2011b; Jones et al., 2010; Lange et al., 2012; Linkenkaer-Hansen et al., 2004; Schubert et al., 2009; Weisz et al., 2014). The inhibitory role of alpha-band activity for neural processing is substantiated by the phase dependence between alpha-band and spiking activity in monkeys and gamma-band activity in humans (Osipova et al., 2008; Haegens et al., 2011b; Spaak et al., 2012; Roux et al., 2013). Furthermore the power of ongoing alpha band activity is inversely correlated with local BOLD-activity (Osipova et al., 2008; Haegens et al., 2011b; Spaak et al., 2012; Roux et al., 2013; Goldman et al., 2002; Moosmann et al., 2003; de Munck et al., 2007; Ritter et al., 2009; Becker et al., 2011), while the relationship between power-fluctuations in alpha- and gamma-band activity seems to be more complex (Hirschmann et al., 2020; Wittenberg et al., 2018). Alpha-band activity seems also to be relevant for top-down processes such as attention in a way, that increases in amplitude can be found for to-be-ignored stimuli or locations (Forschack et al., 2017; Haegens et al., 2011a; Keil et al., 2016; Wöstmann et al., 2017).

Furthermore, the strength of functional network connectivity within different sensory systems was negatively correlated with the power in

* Corresponding authors.
E-mail addresses: christopher.gundlach@uni-leipzig.de (C. Gundlach), sehm@cbs.mpg.de (B. Sehm).

https://doi.org/10.1016/j.neuroimage.2020.117175
Received 29 May 2020; Received in revised form 19 June 2020; Accepted 14 July 2020
Available online 17 July 2020

the alpha-band as found with MEG-recordings for the somatosensory (Weisz et al., 2014) and the auditory system (Leske et al., 2015) and with fMRI for the visual system (Scheeringa et al., 2012). Recently we showed, that imperceptible somatosensory stimulation induces an increase in mu-alpha amplitude (Forschack et al., 2017; Nierhaus et al., 2015) and a functional disconnection of S1 to higher order somatosensory regions (Nierhaus et al., 2015). Fluctuations in alpha-band power, therefore, seem to be related to modulations of information transfer in sensory relevant networks.

While these results are based on correlational findings, techniques like transcranial alternating current stimulation (tACS) may help to elucidate the causal role of alpha-band activity for information processing, by independently modulating oscillations in these frequency bands in various task settings (Thut et al., 2011). Both in vitro (Reato et al., 2010) and in vivo (Helfrich et al., 2014b, 2014a) findings suggest that tACS induces changes in target neural oscillatory activity by entrainment (Lafon et al., 2017; but see Veniero et al., 2015; Vossen et al., 2015). When tACS was applied in the alpha range, behavior was modulated in line with the proposed inhibitory role of alpha-band activity (Jensen and Mazaheri, 2010; Klimesch et al., 2007; Mathewson et al., 2011): auditory, visual and somatosensory perception was dependent on the tACS phase (C. Gundlach et al., 2016; Helfrich et al., 2014b; Neuling et al., 2012a).

Besides changes in local inhibition, the behaviorally relevant effects of alpha-band activity suggest neural interactions on a larger brain scale. Consequently, we here asked, whether modulations of neural activity the alpha-band induce functional connectivity changes on a large-scale brain network level. We specifically examined functional network changes induced by tACS at somatosensory (mu-) alpha frequency (mu-tACS) as measured with resting-state fMRI. Mu-tACS has been shown to modulate the lower frequency part of the mu-rhythm in the alpha-range (8 to 12 Hz) (Gundlach et al., 2017), led to a phasic inhibition of somatosensory perception (C. Gundlach et al., 2016) and changed somatosensory response bias (Craddock et al., 2019). Based on this, we hypothesized a decrease in functional connectivity of left and right primary somatosensory cortex during mu-tACS and expected, that this decrease is specific for mu-tACS and not present when tACS is applied at a physiologically plausible control frequency in the gamma range (65 Hz) (Cheng et al., 2016; Gross et al., 2007; van Ede et al., 2014).

2. Materials and methods

2.1. Participants

20 healthy participants (8 female, mean age 27.85, SD = 3.23) participated in a single-blinded combined fMRI and tACS experiment with a pre-experimental EEG part. All participants were right-handed according to the Oldfield questionnaire for the assessment of handedness (Oldfield, 1971). Prior to the study, participants underwent a neurological examination, were screened for contraindications of participating in non-invasive brain stimulation and MRI experiments and gave written informed consent to participate in the experiment. Participants were not taking any medication. The study was designed and conducted according to the declaration of Helsinki and was approved by the ethics committee of the University of Leipzig.

For a control experiment, a group of 17 healthy, right-handed subjects (7 female, mean age 28.47, SD = 4.17) was invited. The number of participants for the control study was determined by a power analysis based on the central finding of the main experiment. We used G*Power (Faul et al., 2009) to calculate the minimum number of subjects required in order to replicate the central finding from the main experiment (see results: ECM-values decrease during mu-tACS as compared to sham; tested with paired *t*-test; effect size: Cohen's $d = 0.787$) with a power of 0.90 and an alpha probability of 0.05, under the assumption that the found effects are independent of the stimulation frequency. The power analysis revealed a minimum number of 16 subjects.

2.2. Transcranial alternating current stimulation (tACS)

Electric stimulation was delivered with a battery-operated and MRI-compatible stimulator system (ELDITH, Neuroconn, Ilmenau, Germany) via two MRI-compatible rubber electrodes (40 × 40 mm) placed roughly over CCP3 and CCP4 (Oostenveld and Praamstra, 2001) as previously used for bilateral stimulation of both S1 (Gundlach et al., 2017; C. 2016) (see Fig. 1A). The electrodes were connected to the stimulator placed outside the scanner room via cables with 5 kΩ resistors that ran through the scanner room passing a radio frequency filter in the MR cabin wall and with two filter boxes (Neuroconn) placed between stimulator and electrodes in order to reduce potential artifacts during image acquisition. This technical setup has been successfully used before (Sehm et al., 2013, 2012). Impedance was kept below 10 kΩ by applying electrode gel (Ten20, D.O. Weaver, Aurora, CO, USA) between skin and electrode. Stimulation intensity was kept at 1 mA (peak to peak) resulting in a maximum current density of 62.5 μA/cm^2 under the stimulation electrodes.

The corresponding electric field distribution was modeled using a realistic finite element model as implemented in SimNibs 2.0 (Opitz et al., 2015; Thielscher et al., 2015) for illustration for a single subject. For this purpose, from the recorded T1 image different tissue types (white and gray, gray matter, CSF, skin, and skull) were first segmented and tetrahedral volume meshes were then generated using the SimNibs routine. The electric field distribution for a 1 mA direct current (Ruffini et al., 2013) applied with the here used electrode were then modeled and are illustrated in Fig. 1B.

In the main experiment, *verum*-tACS was applied with participants' individual mu-alpha frequency, while in a control study the frequency of the *verum* stimulation was changed to 65 Hz. *Sham* stimulation consisted of noise stimulation of 20 s in length to mimic tingling sensations associated with the onset of real stimulation (Gandiga et al., 2006). For all stimulation blocks the first and last 5 s were ramped up and down in intensity.

2.3. EEG

For the pre-experiment EEG was recorded at a sampling rate of 2500 Hz and a bandpass filter from 0.1 to 1000 Hz using a BrainAmp MR plus amplifier (Brain Products, Munich, Germany) with electrodes placed at positions C3, C4, and POz according to the 10–5 convention (Oostenveld and Praamstra, 2001) (Fig. 1A). Data and electrode impedance levels were recorded using the BrainVision Recorder (Brain Products, Munich, Germany) and impedance levels were always kept below 10 kΩ. The online reference was placed above position FCz and for potential online re-referencing, signals from electrodes above both mastoids were recorded as well. For later offline analysis, EEGLAB (Delorme and Makeig, 2004) and custom Matlab scripts (The MathWorks, Natick, MA, USA) were used, while statistical analyses were performed using R (R Core Team, 2016).

2.4. MRI

All images of the main experiment were recorded with a Siemens Magnetom Tim Trio 3 Tesla scanner and a 32 channel head coil. Due to a hardware-upgrade of the Siemens Magnetom Tim Trio 3 at the time of the scheduled control experiment, this experiment was recorded with a Siemens Magnetom Verio 3 Tesla scanner and a 32 channel head coil.

For resting-state functional imaging a BOLD-contrast sensitive T2*-weighted multiband echo-planar-imaging (EPI) sequence was used (Feinberg et al., 2010; Moeller et al., 2010). Each 18 min and 10 s long resting-state measurement included 1510 whole brain images with 44 slices (AC-PC oriented, multiband factor = 4, data matrix 64 × 64, repetition time (TR) = 722 ms, time echo (TE) = 28 ms, flip angle = 55°, bandwidth = 2003 Hz/Px, field of view (FOV) = 192 mm, resolution = 3 mm x 3 mm x 3 mm, intergap distance = 0.5 mm).

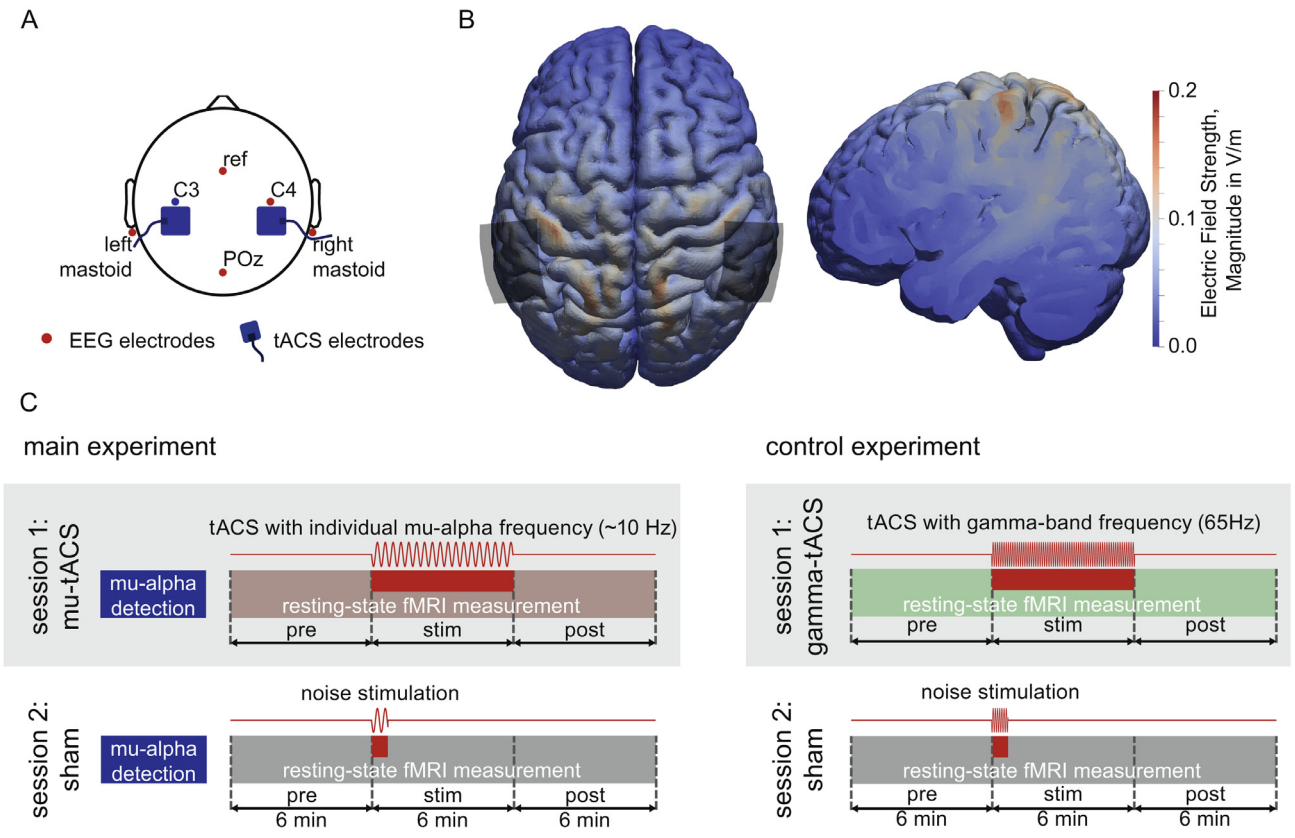

Fig. 1. *Electrode setup, electric field modeling and design for main and control experiment* A) Positioning of EEG electrodes, used in pre-experiment of the main experiment for detection of mu-alpha peak frequencies. TACS electrodes were positioned posterior to C3 and C4, centered approximately at position CCP3 and CCP4. B) Corresponding modeling of electric field strength for 1 mA of applied current for one representative subject. Left: posterior view with electrodes shaded in gray. Right: Sagittal cut at MNI plane of −39 mm illustrating electric field distribution covering left primary somatosensory cortex. C) Procedure for main experiment (mu-tACS applied) and control experiment (gamma-tACS applied). For the main experiment, the resting-state fMRI measurement was preceded by an EEG-experiment in order to determine each participant's individual mu-alpha peak frequency. The sequence of session 1 and session 2 for both experiments was counterbalanced across subjects.

For later spatial coregistration of the functional data, a structural scan was performed by recording T1-weighted images with the MP-RAGE, ADNI-protocol (TR = 2300 ms, TE = 3 ms, time to inversion (TI) = 900 ms, flip angle = 9°, bandwith = 241 Hz/Px, FOV = 256 mm x 240 mm, resolution = 1 mm x 1 mm x 1 mm) (Jack et al., 2008).

2.5. Experimental design

Participants were invited for two sessions that were separated by at least five days. Counterbalanced across subjects, *verum* tACS stimulation was applied on one day and *sham* stimulation on another day. In both sessions, participants were briefed on experimental procedures before EEG and tACS electrodes were mounted. Subsequently, they took part in a pre-experiment in order to determine each participant´s individual mu-alpha peak frequency using EEG and then did the main experiment consisting of a resting-state fMRI measurement.

2.5.1. Pre-experiment

Participants were seated in a comfortable chair inside a shielded EEG chamber while the pre-experiment was conducted to determine each participant's individual mu-alpha peak frequency (10 Hz component of mu-rhythm). Each participant performed a passive somatosensory experiment with simultaneous EEG recording. While participants were fixating a centrally presented cross on a screen, 150 electric suprathreshold stimuli were applied to the right index finger via two Velcro ring-electrodes using a DS7 isolated bipolar constant current stimulator (Digitimer Ltd, Welwyn Garden City, Hertfordshire, UK), with intensity levels set to clearly perceivable but not painful levels. Electric stimuli were delivered with a mean interstimulus interval of 2 s and a maximum jitter of 1 s. The recorded EEG data were then analyzed to extract the Event-Related Desynchronization (ERD) of the mu-rhythm to the presented stimuli (Pfurtscheller et al., 1997; Pfurtscheller and Lopes da Silva, 1999). The frequency with the maximum ERD was identified to serve as the individual target stimulation frequency for the subsequent fMRI-part (see also C. Gundlach et al., 2016).

2.5.2. Main experiment

The main experiment consisted of resting-state functional MRI measurement with a total duration of 18 min and 10 s for which participants were instructed to lie awake, relaxed and motionless with their eyes open. Before the resting-state recording, a fieldmap was recorded to be able to compensate for field inhomogeneities during later data processing. For the resting-state measurement, 1510 images were recorded. After 499 measured volumes (e.g. ~6 min) either *verum*-tACS at participants' individual mu-alpha frequency or *sham*-stimulation was applied (see Fig. 1C). Before and after scanning, subjects were asked to rate their current level of attention, tiredness, and pain on a ten-level visual analog scale. Additionally, after the experiment, participants had to report whether they felt the tACS-stimulation and how sure they were on this (ten-level visual analog scale).

2.5.3. Control experiment

In an independent control experiment, we aimed at testing the specificity of mu-tACS protocol by comparing it with tACS applied in another physiologically plausible frequency range (Gamma, 65 Hz). The second group of subjects was invited for a similar experiment: while the control study had no pre-experiment, it consisted of the same two resting-state fMRI measurements as in the main experiment (see Fig. 1C). However, while the sham stimulation was the same, in the tACS session of the control study tACS was applied with a fixed frequency in the gamma band of 65 Hz bilaterally over both SI.

2.6. Data analysis

2.6.1. Pre-experiment

In order to determine the participants' individual mu-alpha frequency, data recorded at electrode C3 were cut into epochs according to the trigger of the presented stimulus (−1500 ms to +1500 ms). For each trial, signals were wavelet-transformed from 5 to 35 Hz with 0.1 Hz increments using 5 cycle long wavelets to extract the amplitude-time course of various frequencies. A baseline time window from 600 to 300 ms pre-stimulus was subtracted and time courses were averaged across trials to reveal general stimulus-related changes of neural activity for different frequencies. Post-stimulus amplitude values (200 to 600 ms) were then averaged for each frequency. Within the alpha-band (8 to 14 Hz), the frequency with the maximum event-related desynchronization (Pfurtscheller et al., 1997; Pfurtscheller and Lopes da Silva, 1999) i.e., the maximum local amplitude difference between pre- and post-stimulus window, was extracted and served as target stimulation frequency (mu-alpha) for the main experiment. This approach was previously used (Gundlach et al., 2017; C. 2016) and allowed to specifically modulate mu-alpha activity, while not interfering with visual alpha-band activity (see Gundlach et al., 2017).

2.6.2. Main experiment

Preprocessing structural as well as functional images was achieved by using an analysis pipeline, developed and used for resting-state data recorded with a multiband sequence (Feinberg et al., 2010). These preprocessing scripts run in a Python-based Nipype environment (Gorgolewski et al., 2011) under Linux and integrate components of different software platforms, used for preprocessing of functional and structural MRI-data: Freesurfer 5.3.0 (Laboratory for Computational Neuroimaging., 2013), SPM12 (Friston et al., 2007), AFNI (Cox, 1996), ANTS 2.1.0 (Avants, Tustison, Song, et al., 2011; Avants, Tustison, Wu, Cook & Gee, 2011) and FSL 5.0 (Jenkinson, Beckmann, Behrens, Woolrich & Smith, 2012). Code available here (https://github.com/NeuroanatomyAndConnectivity/pipelines/tree/master/src/lsd_lemon).

During preprocessing of the structural data, images were skull-stripped and segmented into gray and white substance with Freesurfer. With ANTS the segmented image was coregistered to an FSL T1 template (MNI coordinate system, 1 mm resolution) and thereby transferred to the standardized MNI space (Evans et al., 1993).

For functional preprocessing, the first 5 images were discarded to allow for initial magnetic stabilization to be complete. Systematic motion in data was extracted as a deviation from the first image. Systematic field inhomogeneities were compensated by using the recorded fieldmaps. Physiological noise and movement artifacts were regressed out. Time courses of BOLD activity were then filtered from 0.01 to 0.1 Hz and data was coregistered to preprocessed structural images and thereby transferred to MNI space. Data were then spatially smoothed with a Gaussian Kernel with 8 mm FWHM for later statistical analysis.

Based on the resulting artifact-corrected and spatially smoothed time course, functional connectivity estimates were calculated for each voxel, each condition (tACS vs sham) and time range (pre-stimulation, stimulation, post-stimulation; each with a length of 499 images) based on the Eigenvector centrality mapping (ECM) (Lohmann et al., 2010) implemented in LIPSIA (Lohmann et al., 2001). ECM is a graph-based, data-driven approach to describe functional network architecture (Zuo et al., 2012). For each voxel, a centrality value is derived based on the degree of functional connectivity. Crucially ECM-values of voxels are high, i.e. are central in the network, if time courses of resting-state BOLD activity measured in theses voxels are correlated with the BOLD activity in many other voxels. Additionally ECM values are scaled if two voxels with correlated activity are themselves central to the network, i.e. their BOLD activity is highly correlated with that in other voxels. Accordingly, low ECM-values are found for voxels with activity less correlated with that of other (central) voxels. For each voxel ECM-values thus evaluate the quantity as well as the quality of its connections. This approach is free of any assumptions on the number of nodes to be used and can be derived for each voxel in the brain. Crucially, while the estimation of ECMs for each voxel allows for identifying central and presumably important nodes in the brain on a network level, by comparing ECM during mu-tACS and sham it is possible to map changes in the network architecture caused by the application of the stimulation. Specifically a potential decrease in centrality in a node during mu-tACS would mean that this node becomes less central to the network by decoupling its activity from that of other (important) nodes in the brain network.

For subsequent statistical testing, the resulting ECM-maps of each subject were transformed to create a normal distribution of these values across all voxels, conditions and time ranges (Lohmann et al., 2010; van Albada and Robinson, 2007).

For testing whether the application of mu-tACS led to an alteration of functional connectivity measures, we planned analyses of changes in Eigenvector centrality (i) in a whole-brain approach and (ii) in predefined regions of interests (ROI) corresponding to the left and right primary somatosensory cortex which were the target regions of tACS. In case of statistically significant changes in these approaches, we planned an additional exploratory seed-based investigation to potentially identify alterations in specific functional connections. Thus online-changes in functional connectivity induced by mu-tACS were investigated on 3 different levels:

First, potential differences in Eigenvector centrality measures between tACS- and sham-session were analyzed in primary somatosensory cortices, the target regions of our tACS protocol in an ROI-approach. Therefore, average Eigenvector centrality indices were extracted for right and left primary somatosensory cortex based on two 9 mm spheres centered at voxels in bilateral cortices (MNI: $x = \pm 40$ mm, $y = -24$ mm, $z = 50$ mm) described in a meta-analysis (Mayka et al., 2006) and differences between tACS and sham application were tested with paired t-test. In addition, differences between tACS- and sham-connectivity measures in both somatosensory cortices were tested for the time window before and after stimulation.

Second, potential changes of Eigenvector centrality in different brain regions were examined with a whole brain approach, as suggested by Cabral Calderin et al. (Y. 2016), who reported connectivity changes due to occipitally applied tACS for brain regions beyond directly stimulated brain areas. For this purpose differences in Eigenvector centrality measures between tACS and sham-stimulation across the whole brain were tested with a paired t-test implemented in AFNI (3dttest++). Resulting z-values were thresholded ($z > 2.576$, e.g. $p < .01$) on a voxel level and corrected on a cluster level ($p < .05$, corrected, based on Monte Carlo simulations implemented in AFNI with 3dClustSim).

Third, specific connectivity changes between the target region in S1 and all other voxels in the brain were tested with a seed-based approach. From a 3 mm sphere centered at the peak-voxel of the previous ECM based analysis, the first eigenvariate of the BOLD-timecourse was extracted (Friston et al., 2006) and used as a regressor for the whole brain activity in a linear regression model implemented with SPM12 (Friston et al., 2007) for each subject. Potential differences in the whole brain connectivity to the seed region were tested with a paired t-test (3dttest++ in AFNI, voxel-wise thresholded at $z > 2.576$, cluster corrected with $p < .05$, one-tailed). With this approach, areas were identified that had significantly lower functional connectivity to the seed

during tACS as compared to sham. Images were created with MRIcron (Rorden et al., 2007).

2.6.3. Control experiment

The analysis of the control experiment was performed analogously to the main experiment as described above. After preprocessing, online-changes in functional connectivity induced by mu-tACS were investigated with 1) an analysis of changes of Eigenvector centrality measures in left S1 during tACS as compared to sham. In order to directly compare results of both studies, a mixed ANOVA model was used to test ECM-values of left S1 with the between-subjects factor STUDY (mu-tACS vs gamma-tACS) and a within-subjects factor SESSION (tACS vs sham), implemented in R (R Core Team, 2016). 2) Potential changes of Eigenvector centrality during gamma-tACS as compared to sham were examined on a whole-brain level. 3) A seed-based connectivity analysis was performed with the same seed as used in the main experiment in order to compare potential connectivity changes during gamma-tACS and mu-tACS. A paired *t*-test with a two-tailed hypothesis was used for comparison of potential changes induced by gamma-tACS vs. sham (3dttest++ in AFNI, voxel-wise thresholded at $z > 2.576$, cluster corrected with $p < .05$, two-tailed).

2.6.4. Subjective ratings

For main and control experiment, the difference between pre/post ratings of attention, vigilance, and pain between tACS and sham blocks were compared with a Wilcoxon Signed Ranks test. Ratings for stimulation perceived vs not perceived for the tACS session compared to the sham session was tested with a McNemar test.

Main Experiment: Overall there were no significant differences between tACS and sham session for any pre- to post-changes of the self-reported variables. Reported vigilance changes (tACS pre: median = 8, ranging from 6 to 10, tACS post: median = 7, ranging from 4 to 10; sham pre: median = 8, ranging from 6 to 10, sham post: median = 8, ranging from 5 to 10) were not significantly different between tACS and sham ($Z = -1.36$, $p = .175$). Neither was there any significant difference of pre- to post-modulation for tiredness ($Z = -1.29$, $p = 0.197$) between tACS (pre: median = 3, range = 1 to 7, post: median = 3, range = 1 to 7) and sham (pre: median = 3, range = 1 to 5, post: median = 3, range = 2 to 6). Pre- to post- differences in ratings of pain level were comparable between tACS and sham session ($Z = 0$; $p = 1$; tACS pre/post: median = 1, range = 1 to 2; sham pre: median = 1, range = 1 to 1; sham post: median = 1, range 1 to 2).There was no significant difference in the reported frequency of skin sensations due to the stimulation between sham and tACS, as revealed by the McNemar test ($p = .065$).

Control Experiment: Consistent with the main experiment, overall there were no significant differences between tACS and sham session for any pre- to post-changes of the self-reported variables. Reported vigilance changes (tACS pre: median = 8, ranging from 7 to 10, tACS post: median = 8, ranging from 5 to 10; sham pre: median = 8, ranging from 6 to 10, sham post: median = 8, ranging from 6 to 9) were not significantly different between tACS and sham ($Z = -0.92$, $p = .356$). There was no significant difference of pre- to post-modulation for tiredness ($Z = -1.09$, $p = .275$) between tACS (pre: median = 2, range = 1 to 4, post: median = 3, range = 1 to 5) and sham (pre: median = 3, range = 1 to 6, post: median = 4, range = 2 to 8). Pre- to post-differences in ratings of pain level were comparable between tACS and sham session ($Z = 0$; $p = 1$; tACS pre: median = 1, range = 1 to 1; post: median = 1, range = 1 to 2; sham pre/post: median = 1, range = 1 to 2). Again, there was no significant difference in the reported frequency of skin sensations due to the stimulation between sham and tACS, as revealed by the McNemar test ($p = .267$).

2.7. Code and data availability

The code used to generate the main findings and the datasets generated during and/or analyzed during the current study are available from the corresponding author upon reasonable request.

3. Results

3.1. Identification of individual mu-alpha stimulation frequencies

Before the actual fMRI-experiment, participants' individual somatosensory mu-alpha frequency was identified based on the event-related desynchronization (ERD) (Pfurtscheller and Lopes da Silva, 1999) to suprathreshold somatosensory stimuli measured with the EEG as used in previous experiments (Gundlach et al., 2017; C. 2016). The peak frequency with the maximum ERD in the alpha range was extracted from signals measured at electrode C3 for 200 to 600 ms post-stimulus. ERD patterns varied in frequency ($M = 10.625$ Hz, $SD = 1.723$) and amplitude across subjects (see Fig. 2B) due to interindividual differences in somatosensory mu-alpha peak frequency. However, when amplitude spectra are aligned to each subject's individual mu-alpha peak frequency, a strong ERD pattern emerges: This pattern is typical for somatosensory processing (Gundlach et al., 2017; C. 2016; Pfurtscheller and Lopes da Silva, 1999) and is characterized by a decrease in amplitude from around 100 to 600 ms post-stimulus for the mu-alpha peak frequency and neighboring frequencies. Additionally, a more transient decrease in the beta range (mu-alpha + around 10 Hz) is followed by a beta rebound (see Fig. 2A).

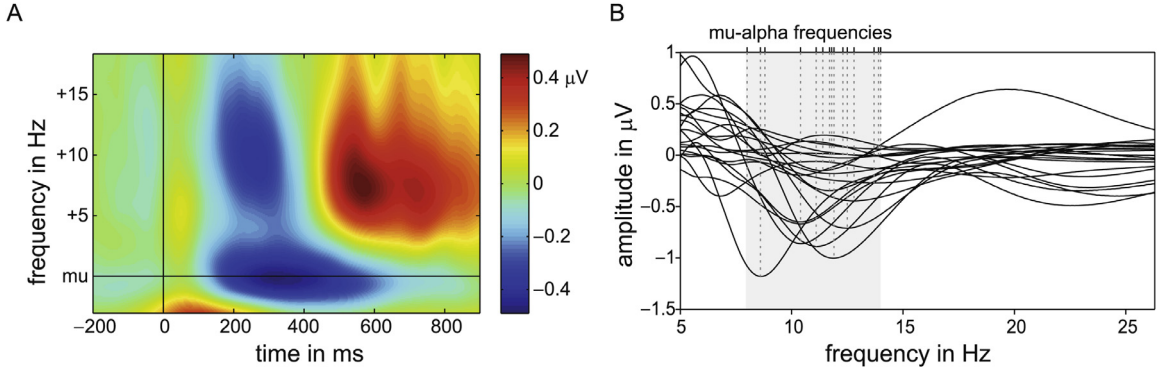

Fig. 2. *ERD patterns of pre-experiment* A) Average, baseline corrected time-frequency plot of signals measured at electrode C3 across all subjects, aligned to each participant's individual mu-alpha frequency and presentation of suprathreshold electric stimuli (at 0 ms). B) Subjects' individual amplitude spectra for the time window averaged from 200 to 600 ms post-stimulus. Dashed lines indicate individual mu-alpha peak frequencies with maximum ERD in the alpha band (8 to 14 Hz, shaded in gray).

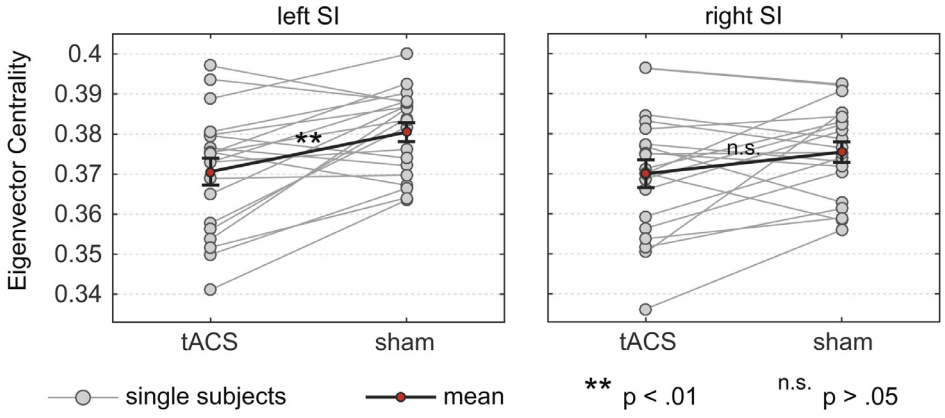

Fig. 3. *Eigenvector centrality measures of left and right primary somatosensory cortices* The Figure represents mean and single subject Eigenvector centrality measures from spheres in primary somatosensory cortex (MNI: x= ±40 mm, y = −24 mm, z = 50 mm) derived from data recorded during tACS and sham stimulation.

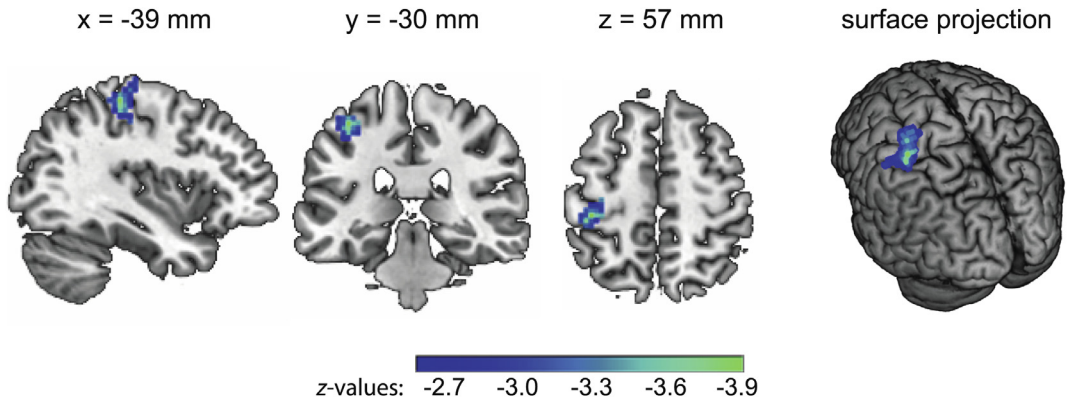

Fig. 4. *Results of whole-brain ECM analysis* The figure represents z-values of a significant cluster for the whole brain comparison of ECM-values for tACS vs sham. The shown cluster shows voxels for which ECM-values were significantly smaller during tACS as compared to sham (voxelwise threshold $|z| > 2.576$, cluster corrected for $p < .05$). The cluster was located in left primary somatosensory and motor cortex.

3.2. Mu-tACS specifically reduces functional connectivity in S1

In a first step we compared Eigenvector centrality measures (ECM), as a marker of the degree of whole-brain connectivity of each voxel in the cortical target areas, the left and right primary somatosensory cortices (MNI: x= ±40 mm, y = −24 mm, z = 50 mm) between tACS and sham stimulation. As visible in Fig. 3, Eigenvector centrality values were significantly lower during mu-tACS as compared to sham in left primary somatosensory cortex (tACS: M = 0.371, SD = 0.015, sham: M = 0.380, SD = 0.011, $t(19) = -3.520$, p = 0.002, d = 0.787). A similar pattern was found on a trend-level for the right somatosensory cortex (tACS: M = 0.370, SD = 0.015, sham: M = 0.375, SD = 0.011, $t(19) = -1.922$, p = 0.070, d = 0.430).

Before stimulation, Eigenvector centrality values neither in left (tACS: M = 0.375, SD = 0.015, sham: M = 0.378, SD= 0.013, $t(19) = -1.141$, p = .268, d = 0.255) nor right primary somatosensory cortex (tACS: M = 0.374, SD = 0.016, sham: M = 0.374, SD = 0.012, $t(19) = -0.173$, p = .864, d = 0.039) were different between tACS and sham. Similarly after stimulation, no significant differences were observable for left (tACS: M = 0.372, SD = 0.015, sham: M = 0.375, SD = 0.011, $t(19) = -1.009$, p = 0.326, d = 0.226) or right S1 (tACS: M = 0.370, SD = 0.015, sham: M = 0.373, SD = 0.013, $t(19) = -0.954$, p = .352, d = 0.213).

The whole brain analysis revealed a specific decrease in Eigenvector centrality during tACS as compared to sham in a single cluster (124 voxels in cluster, peak voxel: MNI coordinates: x = −39 mm, y = −30 mm, z = 57 mm; z-value = −3.897) located in left primary somatosensory cortex (Brodmann area 3b, 1, 2) and left primary motor cortex (Brodmann area 4) according to SPM's anatomy toolbox (Eickhoff et al., 2005) (Fig. 4).

In an additional analysis, we asked, which network might contribute to the overall decrease in Eigenvector centrality in S1. Therefore, using a seed-based connectivity analysis, differences in connectivity strength of the identified region and any other voxel in the brain between tACS and sham was tested. The analysis revealed six clusters for which functional connectivity was significantly reduced during tACS as compared to sham (voxelwise threshold $z > 2.576$, cluster corrected for $p < .05$, one-sided) (see Fig. 5 and Table 1).

3.3. No reduction of S1 functional connectivity during gamma-tACS

In the control study, the application of tACS at a gamma frequency of 65 Hz did not induce changes in Eigenvector centrality as compared to sham in left S1 (tACS: M = 0.371; SD = 0.015; sham: M = 0.369; SD = 0.012; $t(16) = 0.629$; p = 0.538; d = 0.153) or right S1 (tACS: M = 0.367; SD = 0.016; sham: M = 0,368; SD = 0.009; $t(16) = -0.252$; p = 0.805; d = 0.061). For both SI there were no differences before or after stimulation (all ps >0.568). A direct comparison of ECM-values in left S1 across studies with a mixed ANOVA model comprising the between-subject factor STUDY (mu-tACS vs gamma-tACS) and within-subject factor SESSION (tACS vs sham) revealed a main effect for the factor SESSION ($F(1,35) = 4.41$, p = .043, η_g^2 = 0.025), no effect of the factor STUDY ($F(1,35) = 1.88$, p = .179, η_g^2 = 0.041) and crucially a significant interaction ($F(1,35) = 8.73$, p = .006, η_g^2 = 0.048) driven by the significant difference of ECM-values between mu-tACS and sham but not gamma-tACS and sham as stated above.

Interestingly the whole brain analysis revealed one cluster with increased functional connectivity values during tACS as compared to sham (66 voxels in cluster, peak voxel: MNI coordinates: x = 33 mm, y = 0 mm,

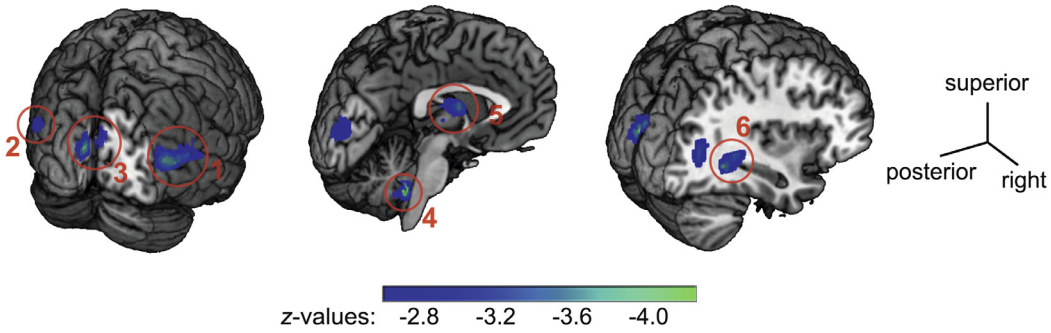

Fig. 5. *Results of seed-based connectivity analysis of the main experiment* The figure represents *z*-values of clusters for which connectivity to a seed region in left primary somatosensory cortex (3 mm sphere, MNI coordinates: $x = -39$ mm, $y = -30$ mm, $z = 57$ mm) was significantly lower during mu-tACS as compared to sham stimulation (voxelwise threshold $|z| > 2.576$, cluster corrected for $p < .05$, one-sided). Clusters are encircled in red with numbers corresponding to cluster number in Table 1. (For interpretation of the references to colour in this figure legend, the reader is referred to the web version of this article.)

Table 1
Clusters that showed a significant reduction in functional connectivity to the seed in left SI during tACS as compared to sham.

no	Peak voxel MNI coordinates (x, y, z) in mm	*z*-values	Number of voxels in cluster	Probabilistic anatomical region
1	60, −72, 12	−3.588	183	right intraparietal cortex
2	−33, −72, 12	−3.475	124	left intraparietal cortex
3	3, −90, 18	−4.072	117	bilateral Cuneus
4	−6, −42, −39	−4.241	65	left cerebellum, Lobule IX, X
5	39, −51, −3	−3.767	63	right middle temporal gyrus
6	0, −3, 15	−3.679	58	left Thalamus

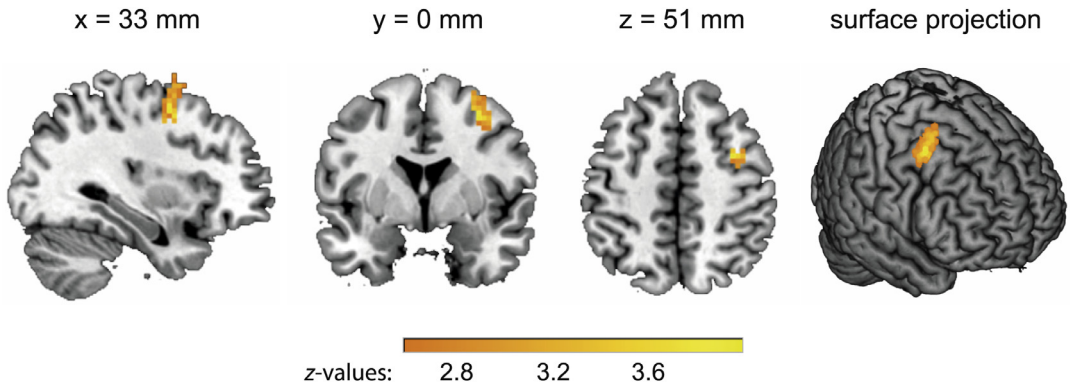

Fig. 6. *Results of whole-brain ECM analysis for the control experiment* The figure represents *z*-values of a significant cluster for the whole brain comparison of ECM-values for tACS applied with 65 Hz vs sham in the control study. The shown cluster shows voxels for which ECM-values were significantly greater during tACS as compared to sham (voxelwise threshold $|z| > 2.576$, cluster corrected for $p < .05$).

Table 2
Clusters that showed a significant reduction in functional connectivity to the seed in left SI during Gamma-tACS as compared to sham.

no	Peak voxel MNI coordinates (x, y, z) in mm	*z*-values	Number of voxels in cluster	Probabilistic anatomical region
1	63, −15, 18	4.456	315	right pre- and postcentral gyrus, operculum, insula
2	−27, −87, −36	−3.727	179	left cerebellum Crus 2 and Crus 1
3	−54, 6, 0	4.121	143	left superior temporal gyrus, insula
4	−51, −3, 27	4.797	98	left precentral and postcentral gyrus

$z = 51$ mm; *z*-value = 3.981) in right dorsolateral prefrontal cortex (Fig. 6).

In order to test the frequency specificity of the seed-based connectivity changes in the main experiment during the application of mu-tACS, a seed-based connectivity analysis with the same seed (3 mm sphere, MNI coordinates: $x = -39$ mm, $y = -30$ mm, $z = 57$ mm) was performed for the control experiment. As can be seen in Table 2 and Fig. 7, the contrast between gamma-tACS and sham revealed a strikingly different pattern as compared to the main experiment with connectivity increases between the seed in left SI and three other brain regions (cluster 1, 3 and 4) as well as connectivity decrease with one brain region in the cerebellum (cluster 2).

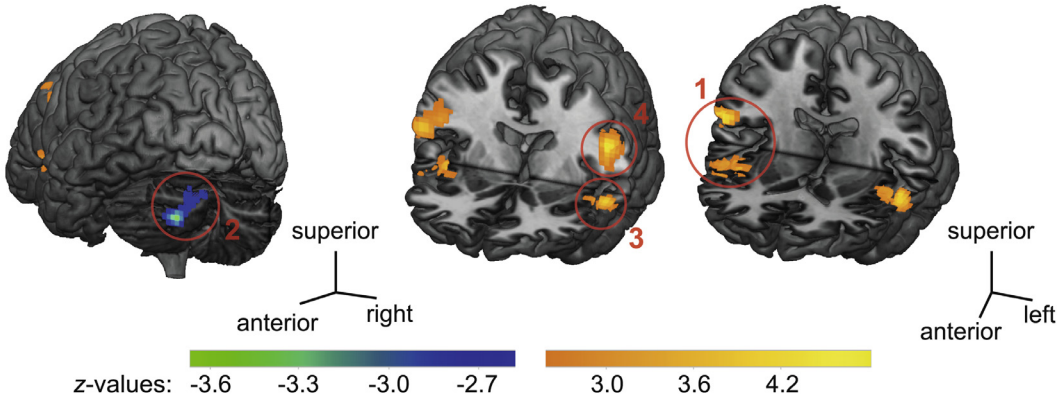

Fig. 7. *Results of seed-based connectivity analysis of the control experiment* The figure represents *z*-values of clusters for which connectivity to a seed region in left primary somatosensory cortex (3 mm sphere, MNI coordinates: $x = -39$ mm, $y = -30$ mm, $z = 57$ mm) was significantly modulated during gamma-tACS as compared to sham stimulation (voxelwise threshold $|z| > 2.576$, cluster corrected for $p < .05$, two-sided). Clusters are encircled in red with numbers corresponding to cluster number in Table 2. (For interpretation of the references to colour in this figure legend, the reader is referred to the web version of this article.)

4. Discussion

We here demonstrate that tACS applied at individual somatosensory mu-alpha frequency induces a decrease in functional connectivity of the primary somatosensory cortex, most likely by entrainment of endogenous oscillatory mu-alpha-band activity. Our results suggest how activity in the alpha-band, the most prominent rhythm of the human brain, may affect activity on a whole-brain network level: by specifically decoupling primary sensory areas as hubs for sensory processing. With our experimental approach, we demonstrate that the application of tACS tuned to endogenous functional rhythms is an avenue to induce local and functionally specific effects on a whole-brain network level.

Our findings support the general notion of a suppressive function of neural alpha-band activity in sensory processing and the gating of information. Multiple studies linking power fluctuations in the alpha-band to changes of neural information flow, have converged to the concept that alpha-band activity represents an inhibitory brain mode for the orchestration of information processing in the brain (Foxe and Snyder, 2011; Jensen and Mazaheri, 2010; see: Klimesch et al., 2007; Palva and Palva, 2007). In this vein, changes in local neural excitability were shown to be linked to the phase and amplitude of alpha-band activity. Specifically, the cyclic nature of alpha-band activity may create inhibitory phases which increase in its temporal extent when alpha-band activity is increased in amplitude. An inhibitory role of this rhythm has been suggested by an inverse correlation between measures of neural activity (gamma in humans; spiking activity in monkeys) and alpha-band amplitude (Haegens et al., 2011b; Osipova et al., 2008; Roux et al., 2013; Spaak et al., 2012). In a similar vein, only recently it was demonstrated that induction of LTP-like neuroplastic changes crucially depends on the phase of ongoing activity in the alpha-band in humans (Zrenner et al., 2018).

Beyond such local aspects of alpha-activity, MEG-studies investigated network-level alpha-band dynamics and demonstrated, that states of low alpha-amplitude are beneficial for stimulus perception and linked to increased functional connectivity measures for corresponding sensory areas (Frey et al., 2016; Leske et al., 2015; Weisz et al., 2014). Similarly, states with low visual alpha-band amplitude were related to pronounced stimulus-driven activity in visual areas and decreased activity in the default mode network as well as auditory areas, assessed with fMRI. Increased alpha-amplitudes, in contrast, reversed the pattern, suggesting a cross-modal regulation of cortical excitation and inhibition within the visual-auditory network by alpha-power fluctuations (Mayhew et al., 2013). Besides these modulations of functional connectivity within a visuo-auditory network, increases in alpha-band power also covaried with a decrease in long-range neural connectivity between the visual cortex and the rest of the brain (Scheeringa et al., 2012) and were related to a gating of visual information to downstream visual areas (Zumer et al., 2014). Our findings strongly support the assumed modulatory role of alpha-band activity on a network level and add causal evidence to previous correlational studies: we show that an externally applied stimulation with a frequency matching the peak frequency of endogenous alpha-band activity, induces changes in functional connectivity of the neuroanatomical substrates of the target somatosensory system. Therefore, we provide evidence that alpha-band activity represents a mechanism for the direct alteration of information transfer and are not only a mere epiphenomenon thereof.

The specificity of this finding was underlined by our control study: the application of tACS at a frequency in the gamma band (65 Hz) did not decrease whole-brain centrality of S1. However, in this experiment, we found increases in Eigenvector centrality values of the right dorsolateral prefrontal cortex (DLPFC) as well as an increase in connectivity between a seed in S1 and a secondary somatosensory and multisensory network during gamma-tACS as compared to sham. These results themselves are interesting in the light of previous studies that 1) link gamma oscillatory activity to cognitive functions (e.g. visuo-spatial working memory, visual image categorization, decision making) with the DLPFC as a relevant hub region (Chand et al., 2016; Haxby et al., 2000). 2) The brain regions for which we found modulation of seed-based connectivity to left S1 during gamma-tACS, such as the cerebellar region, were linked to multisensory integration (Huang et al., 2013; Ishikawa et al., 2015; Rondi-Reig et al., 2014). The regions in the pre- and post-central gyrus, insula and operculum have been associated with upstream somatosensory and somatomotor processing (Mazzola et al., 2006; Preusser et al., 2015) with gamma-band activiy as a relevant brain rhythm for information transfer (Cheng et al., 2016; Hagiwara et al., 2010). These findings additionally confirm that combining tACS with functional MRI is a promising tool for investigating a broad range of brain rhythms and their neuroanatomical and functional substrates.

The differential results between both stimulation conditions (alpha- vs. gamma-frequency) strongly emphasize the frequency dependence of tACS effects. Hence, stimulation effects do not only depend on the locus of the stimulation but rather, based on resonance phenomena, on the interaction of the specific stimulation frequency and the endogenous neural frequencies (Ali et al., 2013; Herrmann et al., 2013; Negahbani et al., 2019; Reato et al., 2013). This approach, to target functionally relevant endogenous rhythms and thus differential neural networks, might, therefore, improve the rather poor spatial and functional specificity of transcranial electric stimulation techniques (Neuling et al., 2012b; Sehm et al., 2013). A previous study demonstrated, that a tACS-based modulation of oscillations in the beta-band at 20 Hz induced a

decrease in functional connectivity between both primary motor cortices (Weinrich et al., 2017). In our study, we used a different stimulation approach, by matching the stimulation frequency to the individual functional (Mu) frequency as assessed in a pre-experiment using EEG. Based on previous findings (Helfrich et al., 2014b; Herrmann et al., 2013; Reato et al., 2013), we reasoned to maximize resonance phenomena and thereby increase potential stimulation effects (see Kasten et al., 2019; Stecher et al., 2017; Stecher and Herrmann, 2018) as well as target the somatosensory system. Indeed, we show that our stimulation protocol specifically modulates connectivity of the target somatosensory system with its central hub, the primary somatosensory cortex.

Interestingly, the seed-based analysis revealed, that the decrease in functional connectivity strength in the primary somatosensory cortex during mu-tACS is most prominently driven by a decrease of connectivity to a network of brain regions that are involved in somatosensory processing and involves thalamus, cuneus, intraparietal cortex, and the cerebellum. Within this network, the thalamus represents a structure that acts as a central hub and gatekeeper of incoming somatosensory information (Patestas and Gartner, 2013; Sherman, 2006). Cuneus, as well as the intraparietal cortex, are regions involved in multisensory integration and processing (Ehrsson et al., 2004; Grefkes et al., 2002; Grefkes and Fink, 2005). Lobule IX and X of the cerebellum were shown to receive somatosensory input necessary for somatomotor processing and integration in rats (Rondi-Reig et al., 2014) and were specifically active during multisensory and sensorimotor processing in humans (Kipping et al., 2013; Stoodley et al., 2012). Taken together, mu-tACS decouples primary somatosensory cortex as a central hub of the somatosensory system from a network of downstream as well as upstream brain regions that are crucially involved in somatosensory and multisensory processing.

For stimulation, we used a bilateral setup centered over both S1. Accordingly, our findings reveal changes in functional connectivity in a bilateral network, however with stronger and significant effects in left S1. One reason for this lateralization of induced changes may be related to the experimental procedure for identifying each subject's individual stimulation frequency: the stimulation frequency was derived from the pre-experiment that was based on stimulation of the right index finger and data extraction from oscillatory dynamics of the left somatosensory cortex. This procedure may thus have tailored the tACS application specifically to the left somatosensory cortex. As mentioned before, stimulation is most effective when endogenous and stimulation frequency match (Ali et al., 2013; Herrmann et al., 2013; Kasten et al., 2019; Negahbani et al., 2019; Reato et al., 2013; Stecher et al., 2017; Stecher and Herrmann, 2018). Since mu-alpha-peak frequencies between left and right somatosensory cortex slightly differ (Pfurtscheller et al., 1977), the stimulation frequency in our study was potentially less optimized for the right somatosensory cortex, which in turn might have resulted in less prominent effects in this brain area.

4.1. Limitations

One potential limitation of our and other studies using tACS study pertains to a recent discussion regarding the underlying mechanisms of stimulation-induced effects. Only recently Asamoah and colleagues (B. 2019) reported that stimulation effects for the motor system may be mediated by transcutaneous stimulation effects rather than by direct transcranial neural modulation. Furthermore, also retinal stimulation effects have been reported (Schutter, 2016), so that various mechanism, including peripheral and central effects, may contribute to the overall outcome of tACS. This is a general discussion regarding tACS that needs to be further elucidated in future studies. However, there are various relevant findings that substantiate a neural source of tACS stimulation effects. First, in own previous work we found a modulation of somatosensory behavior only when tACS was applied with a montage and a stimulation protocol (similar to the one employed here) targeting somatosensory mu-alpha activity but not when tACS was applied in the alpha-band over visual areas (C. Gundlach et al., 2016). This finding would not be expected if a mere transcutaneous stimulation effect were to be hypothesized. Others found that stimulation effects seem to differ and depend on the stimulation montage (Feurra et al., 2011; Krause et al., 2019; Yaple et al., 2017). Furthermore, stimulation effects could be located in areas beyond visual or sensory regions as tACS modulated task-related BOLD activity in frontal working-memory relevant regions directly beneath the tACS electrodes during a working memory task (Violante et al., 2017). Only recently, Kasten et al. (2019) found a link between interindividual differences in anatomy and thus differences in modelled intracranial electric fields and differences in stimulation aftereffects measured with MEG after the application of tACS. A link between interindividual differences in peripheral electric fields in the skin and eyeballs and stimulation aftereffects on the other hand could not be found. Similarly, Negahbani et al. (2019) show some preliminary evidence that in vivo measurements of neural activity in animals during tACS are well in accordance with entrainment-related dynamics of alpha-band activity as modelled in a biologically-motivated thalamo-cortical generative model of neural alpha-activity. In direct response to the work from B. Asamoah et al. (2019) Vieira and colleagues (P.G. 2019) also report preliminary evidence that peripheral somatosensory input is not required for tACS effects on brain activity as neural activity in non-human primates was still entrained by tACS even when somatosensation was blocked or strongly suppressed.

Another limitation of our and other studies using tACS is that a potential entrainment of neural oscillations during the application of mu-tACS cannot be measured directly, but must be inferred. Based on a large body of in-vivo, in-vitro and in-silico experiments in animal models as well as in human experiment using EEG and MEG, there is strong evidence that applied electric oscillatory stimulation leads to entrainment of ongoing neural oscillatory activity during the application (Herrmann et al., 2016, 2013; Krause et al., 2019; Reato et al., 2013) that also manifests in power decreases (Helfrich et al., 2014b; Negahbani et al., 2019). Crucially, in previous work, we found a phasic modulation of somatosensory perception by mu-tACS in accordance with the mechanism of entrainment of neural oscillatory activity during the application of tACS. Stimulation effects outlasting the actual stimulation, may however rely on different mechanisms than mere entrainment and may potentially be related to neural plasticity, rebound and/or homeostasis (Zaehle et al., 2010; Strüber et al., 2015; Veniero et al., 2015; Vossen et al., 2015; Haberbosch et al., 2019). In line with this, we recently found a post-stimulation decrease in mu-alpha amplitude after tACS ceased that is more reconcilable with a plasticity/homeostasis-dependent mechanisms rather than a direct effect related to entrainment (Gundlach et al., 2017). The found decrease in mu-alpha power (in contrast to previous findings of post-tACS alpha-power increases) may point to a particularity of our stimulation protocol. With our montage, directly adopted from an early tACS study (see Zaehle et al., 2010), both primary somatosensory cortices are stimulated antiphasically, potentially leading to metaplastic mechanisms after the anti-phasic stimulation of both SI (Gundlach et al., 2017). How different stimulation montages (e.g. only one stimulation electrode above SI to target either left or right SI only) may affect the modulation of centrality needs to be examined in future studies. Nonetheless, our findings are well in line with the predominantly-hypothesized mechanism of entrainment of mu-alpha activity by mu-tACS. An expected offline post-stimulation effect of mu-tACS on functional connectivity (stemming from a decrease in mu-alpha amplitude as reported previously) (Gundlach et al., 2017), however, was not measurable. This may be due to the fact that decreases in the mu-alpha-band amplitude were transient and only measurable in a two minute long time window while the estimation of centrality required a time window of around six minutes, based on the acquired BOLD signal.

Furthermore, in the current study, we used one target stimulation frequency (individual mu-alpha peak frequency) and one control frequency (gamma) in order to test effects on functional connectivity. In or-

der to allow for a clear estimation of the frequency specificity, an experimentally implemented parametric modulation of the target stimulation frequency would be desirable for future studies. On this notion, there is a recent study that proposes an efficient sampling of the tACS parameter space (see Lorenz et al., 2019). However, in studies like ours, that require the integration of longer data epochs for the extraction of dependent measures (such as rs-fMRI connectivity measures) this is practically impossible. While in the current study, we used 2 control stimulation conditions (sham stimulation and gamma stimulation), future studies should systematically modulate target stimulation frequencies in order to further characterize the specificity of the target frequency.

5. Conclusion

In sum, we demonstrate that tACS adjusted to individual somatosensory alpha frequency induces a specific functional decoupling of the primary somatosensory cortex. Our results provide causal evidence for the inhibitory mechanism of action of alpha-band activity on the level of whole-brain functional networks: by decoupling primary sensory areas as hubs from other the target network. Of note, we show, that tuning stimulation frequencies to endogenous functional rhythms is an effective way to non-invasively induce functionally and locally specific brain changes and that may thus be of grave relevance both for basic and clinical brain research. The idea that the application of tACS induces functionally and locally specific brain changes may be of high relevance for both basic and clinical brain research.

Declaration of Competing Interest

The authors declare no conflict of interest.

CRediT authorship contribution statement

Christopher Gundlach: Conceptualization, Methodology, Software, Investigation, Formal analysis, Visualization, Writing - original draft. **Matthias M. Müller:** Conceptualization, Supervision, Writing - review & editing. **Maike Hoff:** Investigation, Resources. **Patrick Ragert:** Investigation, Resources. **Till Nierhaus:** Software, Resources, Writing - review & editing. **Arno Villringer:** Conceptualization, Funding acquisition, Supervision, Writing - review & editing. **Bernhard Sehm:** Conceptualization, Methodology, Investigation, Supervision, Writing - original draft.

References

Ali, M.M., Sellers, K.K., Fröhlich, F., 2013. Transcranial alternating current stimulation modulates large-scale cortical network activity by network resonance. J. Neurosci. 33, 11262–11275. doi:10.1523/JNEUROSCI.5867-12.2013.

Asamoah, B., Khatoun, A., Laughlin, M.M., 2019. tACS motor system effects can be caused by transcutaneous stimulation of peripheral nerves. Nat. Commun. 10, 266. doi:10.1038/s41467-018-08183-w.

Becker, R., Reinacher, M., Freyer, F., Villringer, A., Ritter, P., 2011. How Ongoing Neuronal Oscillations Account for Evoked fMRI Variability. J. Neurosci. 31, 11016–11027. doi:10.1523/jneurosci.0210-11.2011.

Buzsáki, G., Draguhn, A., 2004. Neuronal oscillations in cortical networks. ScienceScience 304, 1926–1929. doi:10.1126/science.1099745.

Cabral-Calderin, Y., Williams, K.A., Opitz, A., Dechent, P., Wilke, M., 2016. Transcranial alternating current stimulation modulates spontaneous low frequency fluctuations as measured with fMRI. NeuroimageNeuroimage 141, 88–107. doi:10.1016/j.neuroimage.2016.07.005.

Chand, G.B., Lamichhane, B., Dhamala, M., 2016. Face or House Image Perception: beta and Gamma Bands of Oscillations in Brain Networks Carry Out Decision-Making. Brain Connect 6, 621–631. doi:10.1089/brain.2016.0421.

Cheng, C.-H., Chan, P.-Y.S., Niddam, D.M., Tsai, S.-Y., Hsu, S.-C., Liu, C.-Y., 2016. Sensory gating, inhibition control and gamma oscillations in the human somatosensory cortex. Sci. Rep. 6. doi:10.1038/srep20437.

Craddock, M., Klepousniotou, E., El-Deredy, W., Poliakoff, E., Lloyd, D., 2019. Transcranial alternating current stimulation at 10 Hz modulates response bias in the somatic signal detection task. Int. J. Psychophysiol. Off. J. Int. Organ. Psychophysiol. 135, 106–112. doi:10.1016/j.ijpsycho.2018.12.001.

de Munck, J.C., Gonçalves, S.I., Huijboom, L., Kuijer, J.P.A., Pouwels, P.J.W., Heethaar, R.M., Lopes da Silva, F.H., 2007. The hemodynamic response of the alpha rhythm: an EEG/fMRI study. NeuroimageNeuroimage 35, 1142–1151. doi:10.1016/j.neuroimage.2007.01.022.

Delorme, A., Makeig, S., 2004. EEGLAB: an open source toolbox for analysis of single-trial EEG dynamics including independent component analysis. J. Neurosci. Methods 134, 9–21. doi:10.1016/j.jneumeth.2003.10.009.

Ehrsson, H.H., Spence, C., Passingham, R.E., 2004. That's My Hand! Activity in Premotor Cortex Reflects Feeling of Ownership of a Limb. ScienceScience 305, 875–877. doi:10.1126/science.1097011.

Eickhoff, S.B., Stephan, K.E., Mohlberg, H., Grefkes, C., Fink, G.R., Amunts, K., Zilles, K., 2005. A new SPM toolbox for combining probabilistic cytoarchitectonic maps and functional imaging data. NeuroimageNeuroimage 25, 1325–1335. doi:10.1016/j.neuroimage.2004.12.034.

Ergenoglu, T., Demiralp, T., Bayraktaroglu, Z., Ergen, M., Beydagi, H., Uresin, Y., 2004. Alpha rhythm of the EEG modulates visual detection performance in humans. Cogn. Brain Res. 20, 376–383. doi:10.1016/j.cogbrainres.2004.03.009.

Evans, A.C., Collins, D.L., Mills, S.R., Brown, E.D., Kelly, R.L., Peters, T.M., 1993. 3D statistical neuroanatomical models from 305 MRI volumes, in: nuclear science symposium and medical imaging conference, 1993. In: 1993 IEEE Conference Record. Presented at the Nuclear Science Symposium and Medical Imaging Conference, 1993., 1993 IEEE Conference Record., 3, pp. 1813–1817. doi:10.1109/NSSMIC.1993.373602.

Faul, F., Erdfelder, E., Buchner, A., Lang, A.-G., 2009. Statistical power analyses using G*Power 3.1: tests for correlation and regression analyses. Behav. Res. Methods 41, 1149–1160. doi:10.3758/BRM.41.4.1149.

Feinberg, D.A., Moeller, S., Smith, S.M., Auerbach, E., Ramanna, S., Glasser, M.F., Miller, K.L., Ugurbil, K., Yacoub, E., 2010. Multiplexed echo planar imaging for subsecond whole brain FMRI and fast diffusion imaging. PLoS ONE 5. doi:10.1371/journal.pone.0015710.

Feurra, M., Bianco, G., Santarnecchi, E., Del Testa, M., Rossi, A., Rossi, S., 2011. Frequency-dependent tuning of the human motor system induced by transcranial oscillatory potentials. J. Neurosci. 31, 12165–12170. doi:10.1523/JNEUROSCI.0978-11.2011.

Forschack, N., Nierhaus, T., Müller, M.M., Villringer, A., 2017. Alpha-band brain oscillations shape the processing of perceptible as well as imperceptible somatosensory stimuli during selective attention. J. Neurosci. 2582. doi:10.1523/JNEUROSCI.2582-16.2017, 16https://doi.org/.

Foxe, J.J., Snyder, A.C., 2011. The role of alpha-band brain oscillations as a sensory suppression mechanism during selective attention. Percept. Sci. 2, 154. doi:10.3389/fpsyg.2011.00154.

Frey, J.N., Ruhnau, P., Leske, S., Siegel, M., Braun, C., Weisz, N., 2016. The tactile window to consciousness is characterized by frequency-specific integration and segregation of the primary somatosensory cortex. Sci. Rep. 6, 20805. doi:10.1038/srep20805.

Friston, K.J., Ashburner, J., Kiebel, S., Nichols, T., Penny, W.D., 2007. Statistical Parametric Mapping the Analysis of Funtional Brain Images. Elsevier/Academic Press, Amsterdam; Boston.

Friston, K.J., Rotshtein, P., Geng, J.J., Sterzer, P., Henson, R.N., 2006. A critique of functional localisers. Neuroimage 30, 1077–1087. doi:10.1016/j.neuroimage.2005.08.012.

Gandiga, P.C., Hummel, F.C., Cohen, L.G., 2006. Transcranial DC stimulation (tDCS): a tool for double-blind sham-controlled clinical studies in brain stimulation. Clin. Neurophysiol. 117, 845–850. doi:10.1016/j.clinph.2005.12.003.

Goldman, R.I., Stern, J.M., Engel, J.J., Cohen, M.S., 2002. Simultaneous EEG and fMRI of the alpha rhythm. Neuroreport 13, 2487–2492.

Grefkes, C., Fink, G.R., 2005. REVIEW: the functional organization of the intraparietal sulcus in humans and monkeys. J. Anat. 207, 3–17. doi:10.1111/j.1469-7580.2005.00426.x.

Grefkes, C., Weiss, P.H., Zilles, K., Fink, G.R., 2002. Crossmodal processing of object features in human anterior intraparietal cortex: an fMRI study implies equivalencies between humans and monkeys. Neuron 35, 173–184. doi:10.1016/S0896-6273(02)00741-9.

Gross, J., Schnitzler, A., Timmermann, L., Ploner, M., 2007. Gamma oscillations in human primary somatosensory cortex reflect pain perception. PLOS Biol. 5, e133. doi:10.1371/journal.pbio.0050133.

Gundlach, C., Müller, M.M., Nierhaus, T., Villringer, A., Sehm, B., 2017. Modulation of somatosensory alpha rhythm by transcranial alternating current stimulation at mu-frequency. Front. Hum. Neurosci. 11. doi:10.3389/fnhum.2017.00432.

Gundlach, C., Müller, M.M., Nierhaus, T., Villringer, A., Sehm, B., 2016. Phasic modulation of human somatosensory perception by transcranially applied oscillating currents. Brain Stimulat. 9, 712–719. doi:10.1016/j.brs.2016.04.014.

Haberbosch, L., Schmidt, S., Jooss, A., Köhn, A., Kozarzewski, L., Rönnefarth, M., Scholz, M., Brandt, S.A., 2019. Rebound or entrainment? The influence of alternating current stimulation on individual alpha. Front. Hum. Neurosci. 13. doi:10.3389/fnhum.2019.00043.

Haegens, S., Händel, B.F., Jensen, O., 2011a. Top-down controlled alpha band activity in somatosensory areas determines behavioral performance in a discrimination task. J. Neurosci. 31, 5197–5204. doi:10.1523/JNEUROSCI.5199-10.2011.

Haegens, S., Nácher, V., Luna, R., Romo, R., Jensen, O., 2011b. α-Oscillations in the monkey sensorimotor network influence discrimination performance by rhythmical inhibition of neuronal spiking. Proc. Natl. Acad. Sci. 108, 19377–19382. doi:10.1073/pnas.1117190108.

Hagiwara, K., Okamoto, T., Shigeto, H., Ogata, K., Somehara, Y., Matsushita, T., Kira, J., Tobimatsu, S., 2010. Oscillatory gamma synchronization binds the primary and secondary somatosensory areas in humans. NeuroimageNeuroimage 51, 412–420. doi:10.1016/j.neuroimage.2010.02.001.

Haxby, J.V., Petit, L., Ungerleider, L.G., Courtney, S.M., 2000. Distinguishing the functional roles of multiple regions in distributed neural systems for visual working memory. NeuroimageNeuroimage 11, 380–391. doi:10.1006/nimg.2000.0592.

Helfrich, R.F., Knepper, H., Nolte, G., Strüber, D., Rach, S., Herrmann, C.S., Schneider, T.R., Engel, A.K., 2014a. Selective Modulation of Interhemispheric Func-

tional Connectivity by HD-tACS Shapes Perception. PLoS Biol. 12, e1002031. doi:10.1371/journal.pbio.1002031.
Helfrich, R.F., Schneider, T.R., Rach, S., Trautmann-Lengsfeld, S.A., Engel, A.K., Herrmann, C.S., 2014b. Entrainment of brain oscillations by transcranial alternating current stimulation. Curr. Biol. 24, 333–339. doi:10.1016/j.cub.2013.12.041.
Herrmann, C.S., Murray, M.M., Ionta, S., Hutt, A., Lefebvre, J., 2016. Shaping intrinsic neural oscillations with periodic stimulation. J. Neurosci. 36, 5328–5337. doi:10.1523/JNEUROSCI.0236-16.2016.
Herrmann, C.S., Rach, S., Neuling, T., Struber, D., 2013. Transcranial alternating current stimulation: a review of the underlying mechanisms and modulation of cognitive processes. Front. Hum. Neurosci. 7, 279. doi:10.3389/fnhum.2013.00279.
Hirschmann, J., Baillet, S., Woolrich, M., Schnitzler, A., Vidaurre, D., Florin, E., 2020. Spontaneous network activity <35 Hz accounts for variability in stimulus-induced gamma responses. Neuroimage 207, 116374. doi:10.1016/j.neuroimage.2019.116374.
Huang, C.-C., Sugino, K., Shima, Y., Guo, C., Bai, S., Mensh, B.D., Nelson, S.B., Hantman, A.W., 2013. Convergence of pontine and proprioceptive streams onto multimodal cerebellar granule cells. Elife 2. doi:10.7554/eLife.00400.
Ishikawa, T., Shimuta, M., Häusser, M., 2015. Multimodal sensory integration in single cerebellar granule cells in vivo. Elife 4. doi:10.7554/eLife.12916.
Jack, C.R., Bernstein, M.A., Fox, N.C., Thompson, P., Alexander, G., Harvey, D., Borowski, B., Britson, P.J., Whitwell, J.L., Ward, C., Dale, A.M., Felmlee, J.P., Gunter, J.L., Hill, D.L.G., Killiany, R., Schuff, N., Fox-Bosetti, S., Lin, C., Studholme, C., DeCarli, C.S., Krueger, G., Ward, H.A., Metzger, G.J., Scott, K.T., Mallozzi, R., Blezek, D., Levy, J., Debbins, J.P., Fleisher, A.S., Albert, M., Green, R., Bartzokis, G., Glover, G., Mugler, J., Weiner, M.W., 2008. The Alzheimer's disease neuroimaging initiative (ADNI): MRI methods. J. Magn. Reson. Imaging JMRI 27, 685–691. doi:10.1002/jmri.21049.
Jensen, O., Mazaheri, A., 2010. Shaping functional architecture by oscillatory alpha activity: gating by inhibition. Front. Hum. Neurosci. 5, 12. doi:10.3389/fnhum.2010.00186.
Jones, S.R., Kerr, C.E., Wan, Q., Pritchett, D.L., Hamalainen, M., Moore, C.I., 2010. Cued spatial attention drives functionally relevant modulation of the mu rhythm in primary somatosensory cortex. J. Neurosci. 30, 13760–13765. doi:10.1523/JNEUROSCI.2969-10.2010.
Kasten, F.H., Duecker, K., Maack, M.C., Meiser, A., Herrmann, C.S., 2019. Integrating electric field modeling and neuroimaging to explain inter-individual variability of tACS effects. Nat. Commun. 10, 1–11. doi:10.1038/s41467-019-13417-6.
Keil, J., Pomper, U., Senkowski, D., 2016. Distinct patterns of local oscillatory activity and functional connectivity underlie intersensory attention and temporal prediction. Cortex, What's your poison? Neurobehav. Consequences Exposure Ind. Agricult. Environ. Chem. 74, 277–288. doi:10.1016/j.cortex.2015.10.023.
Kipping, J.A., Grodd, W., Kumar, V., Taubert, M., Villringer, A., Margulies, D.S., 2013. Overlapping and parallel cerebello-cerebral networks contributing to sensorimotor control: an intrinsic functional connectivity study. NeuroimageNeuroimage 83, 837–848. doi:10.1016/j.neuroimage.2013.07.027.
Klimesch, W., Sauseng, P., Hanslmayr, S., 2007. EEG alpha oscillations: the inhibition-timing hypothesis. Brain Res. Rev. 53, 63–88. doi:10.1016/j.brainresrev.2006.06.003.
Krause, M.R., Vieira, P.G., Csorba, B.A., Pilly, P.K., Pack, C.C., 2019. Transcranial alternating current stimulation entrains single-neuron activity in the primate brain. Proc. Natl. Acad. Sci. 116, 5747–5755. doi:10.1073/pnas.1815958116.
Lafon, B., Henin, S., Huang, Y., Friedman, D., Melloni, L., Thesen, T., Doyle, W., Buzsáki, G., Devinsky, O., Parra, L.C., Liu, A., 2017. Low frequency transcranial electrical stimulation does not entrain sleep rhythms measured by human intracranial recordings. Nat. Commun. 8, 1199. doi:10.1038/s41467-017-01045-x.
Lange, J., Halacz, J., van Dijk, H., Kahlbrock, N., Schnitzler, A., 2012. Fluctuations of prestimulus oscillatory power predict subjective perception of tactile simultaneity. Cereb. Cortex 22, 2564–2574. doi:10.1093/cercor/bhr329.
Leske, S., Ruhnau, P., Frey, J., Lithari, C., Müller, N., Hartmann, T., Weisz, N., 2015. Prestimulus network integration of auditory cortex predisposes near-threshold perception independently of local excitability. Cereb. Cortex Bhv. 212. doi:10.1093/cercor/bhv212.
Linkenkaer-Hansen, K., Nikulin, V.V., Palva, S., Ilmoniemi, R.J., Palva, J.M., 2004. Prestimulus oscillations enhance psychophysical performance in humans. J. Neurosci. 24, 10186–10190. doi:10.1523/JNEUROSCI.2584-04.2004.
Lohmann, G., Margulies, D.S., Horstmann, A., Pleger, B., Lepsien, J., Goldhahn, D., Schloegl, H., Stumvoll, M., Villringer, A., Turner, R., 2010. Eigenvector Centrality Mapping for Analyzing Connectivity Patterns in fMRI Data of the Human Brain. PLoS ONE 5, e10232. doi:10.1371/journal.pone.0010232.
Lohmann, G., Müller, K., Bosch, V., Mentzel, H., Hessler, S., Chen, L., Zysset, S., Cramon, D.Y.von, 2001. Lipsia—A new software system for the evaluation of functional magnetic resonance images of the human brain. Comput. Med. Imaging Graph. 25, 449–457. doi:10.1016/S0895-6111(01)00008-8.
Lorenz, R., Simmons, L.E., Monti, R.P., Arthur, J.L., Limal, S., Laakso, I., Leech, R., Violante, I.R., 2019. Efficiently searching through large tACS parameter spaces using closed-loop Bayesian optimization. Brain Stimulat 12, 1484–1489. doi:10.1016/j.brs.2019.07.003.
Mathewson, K.E., Lleras, A., Beck, D.M., Fabiani, M., Ro, T., Gratton, G., 2011. Pulsed Out of Awareness: EEG Alpha oscillations represent a pulsed inhibition of ongoing cortical processing. Front. Psychol. 2. doi:10.3389/fpsyg.2011.00099.
Mayhew, S.D., Ostwald, D., Porcaro, C., Bagshaw, A.P., 2013. Spontaneous EEG alpha oscillation interacts with positive and negative BOLD responses in the visual–auditory cortices and default-mode network. Neuroimage 76, 362–372. doi:10.1016/j.neuroimage.2013.02.070.
Mayka, M.A., Corcos, D.M., Leurgans, S.E., Vaillancourt, D.E., 2006. Three-dimensional locations and boundaries of motor and premotor cortices as defined by functional brain imaging: a meta-analysis. Neuroimage 31, 1453–1474. doi:10.1016/j.neuroimage.2006.02.004.
Mazzola, L., Isnard, J., Mauguière, F., 2006. Somatosensory and Pain Responses to Stimulation of the Second Somatosensory Area (SII) in Humans. A Comparison with SI and Insular Responses. Cereb. Cortex 16, 960–968. doi:10.1093/cercor/bhj038.
Moeller, S, Yacoub, E, Olman, CA, Auerbach, E, Strupp, J, Narel, N, Uğurbil, K, 2010. Multiband multislice GE-EPI at 7 tesla, with 16-fold acceleration using partial parallel imaging with application to high spatial and temporal whole-brain fMRI. Magn. Reson. Med. 63 (5), 1144–1153. doi:10.1002/mrm.22361.
Moosmann, M., Ritter, P., Krastel, I., Brink, A., Thees, S., Blankenburg, F., Taskin, B., Obrig, H., Villringer, A., 2003. Correlates of alpha rhythm in functional magnetic resonance imaging and near infrared spectroscopy. NeuroimageNeuroimage 20, 145–158. doi:10.1016/S1053-8119(03)00344-6.
Negahbani, E., Stitt, I.M., Davey, M., Doan, T.T., Dannhauer, M., Hoover, A.C., Peterchev, A.V., Radtke-Schuller, S., Fröhlich, F., 2019. Transcranial Alternating Current Stimulation (tACS) Entrains Alpha Oscillations by Preferential Phase Synchronization of Fast-Spiking Cortical Neurons to Stimulation Waveform. bioRxiv, 563163 doi:10.1101/563163.
Neuling, T., Rach, S., Wagner, S., Wolters, C.H., Herrmann, C.S., 2012a. Good vibrations: oscillatory phase shapes perception. Neuroimage 63, 771–778. doi:10.1016/j.neuroimage.2012.07.024.
Neuling, T., Wagner, S., Wolters, C.H., Zaehle, T., Herrmann, C.S., 2012b. Finite-element model predicts current density distribution for clinical applications of tDCS and tACS. Front Psychiatry 3, 83. doi:10.3389/fpsyt.2012.00083.
Nierhaus, T., Forschack, N., Piper, S.K., Holtze, S., Krause, T., Taskin, B., Long, X., Stelzer, J., Margulies, D.S., Steinbrink, J., Villringer, A., 2015. Imperceptible somatosensory stimulation alters sensorimotor background rhythm and connectivity. J. Neurosci. 35, 5917–5925. doi:10.1523/JNEUROSCI.3806-14.2015.
Oldfield, R.C., 1971. The assessment and analysis of handedness: the Edinburgh inventory. NeuropsychologiaNeuropsychologia 9, 97–113.
Oostenveld, R., Praamstra, P., 2001. The five percent electrode system for high-resolution EEG and ERP measurements. Clin. Neurophysiol. 112, 713–719. doi:10.1016/S1388-2457(00)00527-7.
Opitz, A., Paulus, W., Will, S., Antunes, A., Thielscher, A., 2015. Determinants of the electric field during transcranial direct current stimulation. Neuroimage 109, 140–150. doi:10.1016/j.neuroimage.2015.01.033.
Osipova, D., Hermes, D., Jensen, O., 2008. Gamma power is phase-locked to posterior alpha activity. PLoS ONE 3, e3990. doi:10.1371/journal.pone.0003990.
Palva, S., Palva, J.M., 2007. New vistas for [alpha]-frequency band oscillations. Trends Neurosci. 30, 150–158. doi:10.1016/j.tins.2007.02.001.
Patestas, M., Gartner, L.P., 2013. A Textbook of Neuroanatomy. John Wiley & Sons, New York, NY.
Pfurtscheller, G., Lopes da Silva, F.H., 1999. Event-related EEG/MEG synchronization and desynchronization: basic principles. Clin. Neurophysiol. 110, 1842–1857. doi:10.1016/s1388-2457(99)00141-8.
Pfurtscheller, G., Maresch, H., Schuy, S., 1977. Inter- and intrahemispheric differences in the peak frequency of rhythmic activity within the alpha band. Electroencephalogr. Clin. Neurophysiol. 42, 77–83. doi:10.1016/0013-4694(77)90152-3.
Pfurtscheller, G., Neuper, C., Andrew, C., Edlinger, G., 1997. Foot and hand area mu rhythms. Int. J. Psychophysiol. 26, 121–135. doi:10.1016/s0167-8760(97)00760-5.
Preusser, S., Thiel, S.D., Rook, C., Roggenhofer, E., Kosatschek, A., Draganski, B., Blankenburg, F., Driver, J., Villringer, A., Pleger, B., 2015. The perception of touch and the ventral somatosensory pathway. Brain 138, 540–548. doi:10.1093/brain/awu370.
R Core Team, 2016. R: A Language and Environment for Statistical Computing. R Foundation for Statistical Computing, Vienna, Austria.
Reato, D., Rahman, A., Bikson, M., Parra, L.C., 2013. Effects of weak transcranial alternating current Stimulation on brain activity – a review of known mechanisms from animal studies. Front. Hum. Neurosci. 7. doi:10.3389/fnhum.2013.00687.
Reato, D., Rahman, A., Bikson, M., Parra, L.C., 2010. Low-intensity electrical stimulation affects network dynamics by modulating population rate and spike timing. J. Neurosci. 30, 15067–15079. doi:10.1523/JNEUROSCI.2059-10.2010.
Ritter, P., Moosmann, M., Villringer, A., 2009. Rolandic alpha and beta EEG rhythms' strengths are inversely related to fMRI-BOLD signal in primary somatosensory and motor cortex. Hum. Brain Mapp. 30, 1168–1187. doi:10.1002/hbm.20585.
Rondi-Reig, L., Paradis, A.-.L., Lefort, J.M., Babayan, B.M., Tobin, C., 2014. How the cerebellum may monitor sensory information for spatial representation. Front. Syst. Neurosci. 8. doi:10.3389/fnsys.2014.00205.
Rorden, C., Karnath, H.-.O., Bonilha, L., 2007. Improving lesion-symptom mapping. J. Cogn. Neurosci 19, 1081–1088. doi:10.1162/jocn.2007.19.7.1081.
Roux, F., Wibral, M., Singer, W., Aru, J., Uhlhaas, P.J., 2013. The phase of thalamic alpha activity modulates cortical gamma-band activity: evidence from resting-state MEG recordings. J. Neurosci. 33, 17827–17835. doi:10.1523/jneurosci.5778-12.2013.
Ruffini, G., Wendling, F., Merlet, I., Molaee-Ardekani, B., Mekonnen, A., Salvador, R., Soria-Frisch, A., Grau, C., Dunne, S., Miranda, P.C., 2013. Transcranial current brain stimulation (tcs): models and technologies. IEEE Trans. Neural Syst. Rehabil. Eng. 21, 333–345. doi:10.1109/TNSRE.2012.2200046.
Samaha, J., Iemi, L., Postle, B.R., 2017. Prestimulus alpha-band power biases visual discrimination confidence, but not accuracy. Conscious. Cogn. 54, 47–55. doi:10.1016/j.concog.2017.02.005.
Scheeringa, R., Petersson, K.M., Kleinschmidt, A., Jensen, O., Bastiaansen, M.C., 2012. EEG alpha power modulation of FMRI resting-state connectivity. Brain Connect 2, 254–264. doi:10.1089/brain.2012.0088.
Schubert, R., Haufe, S., Blankenburg, F., Villringer, A., Curio, G., 2009. Now you'll feel it, now you won't: EEG rhythms predict the effectiveness of perceptual masking. J. Cogn. Neurosci. 21, 2407–2419. doi:10.1162/jocn.2008.21174.
Schutter, D.J.L.G., 2016. Cutaneous retinal activation and neural entrainment in

transcranial alternating current stimulation: a systematic review. NeuroImage. doi:10.1016/j.neuroimage.2015.09.067.

Sehm, B., Kipping, J.A., Schaefer, A., Villringer, A., Ragert, P., 2013. A comparison between uni- and bilateral tDCS effects on functional connectivity of the human motor cortex. Front. Hum. Neurosci. 7, 183. doi:10.3389/fnhum.2013.00183.

Sehm, B., Schafer, A., Kipping, J., Margulies, D., Conde, V., Taubert, M., Villringer, A., Ragert, P., 2012. Dynamic modulation of intrinsic functional connectivity by transcranial direct current stimulation. J. Neurophysiol. 108, 3253–3263. doi:10.1152/jn.00606.2012.

Sherman, S., 2006. Thalamus. Scholarpedia 1, 1583. doi:10.4249/scholarpedia.1583.

Spaak, E., Bonnefond, M., Maier, A., Leopold, D.A., Jensen, O., 2012. Layer-Specific Entrainment of Gamma-Band Neural Activity by the Alpha Rhythm in Monkey Visual Cortex. Curr. Biol. 22, 2313–2318. doi:10.1016/j.cub.2012.10.020.

Stecher, H.I., Herrmann, C.S., 2018. Absence of alpha-tACS aftereffects in darkness reveals importance of taking derivations of stimulation frequency and individual alpha variability into account. Front. Psychol. 9. doi:10.3389/fpsyg.2018.00984.

Stecher, H.I., Pollok, T.M., Strüber, D., Sobotka, F., Herrmann, C.S., 2017. Ten minutes of α-tACS and ambient illumination independently modulate EEG α-power. Front. Hum. Neurosci. 11. doi:10.3389/fnhum.2017.00257.

Stoodley, C.J., Valera, E.M., Schmahmann, J.D., 2012. Functional topography of the cerebellum for motor and cognitive tasks: an fMRI study. NeuroimageNeuroimage 59, 1560–1570. doi:10.1016/j.neuroimage.2011.08.065.

Strauß, A., Henry, M.J., Scharinger, M., Obleser, J., 2015. Alpha phase determines successful lexical decision in noise. J. Neurosci. 35, 3256–3262. doi:10.1523/JNEUROSCI.3357-14.2015.

Strüber, D., Rach, S., Neuling, T., Herrmann, C.S., 2015. On the possible role of stimulation duration for after-effects of transcranial alternating current stimulation. Front. Cell. Neurosci. 311. doi:10.3389/fncel.2015.00311.

Thielscher, A., Antunes, A., Saturnino, G.B., 2015. Field modeling for transcranial magnetic stimulation: a useful tool to understand the physiological effects of TMS? In: 2015 37th Annual International Conference of the IEEE Engineering in Medicine and Biology Society (EMBC). Presented at the 2015 37th Annual International Conference of the IEEE Engineering in Medicine and Biology Society (EMBC), pp. 222–225. doi:10.1109/EMBC.2015.7318340.

Thut, G., Schyns, P.G., Gross, J., 2011. Entrainment of perceptually relevant brain oscillations by non-invasive rhythmic stimulation of the human brain. Front. Psychol. 2, 170. doi:10.3389/fpsyg.2011.00170.

van Albada, S.J., Robinson, P.A., 2007. Transformation of arbitrary distributions to the normal distribution with application to EEG test–retest reliability. J. Neurosci. Methods 161, 205–211. doi:10.1016/j.jneumeth.2006.11.004.

van Dijk, H., Schoffelen, J.-.M., Oostenveld, R., Jensen, O., 2008. Prestimulus oscillatory activity in the alpha band predicts visual discrimination ability. J. Neurosci. 28, 1816–1823. doi:10.1523/jneurosci.1853-07.2008.

van Ede, F., Szebenyi, S., Maris, E., 2014. Attentional modulations of somatosensory alpha, beta and gamma oscillations dissociate between anticipation and stimulus processing. Neuroimage 97, 134–141. doi:10.1016/j.neuroimage.2014.04.047.

Veniero, D., Vossen, A., Gross, J., Thut, G., 2015. Lasting EEG/MEG aftereffects of rhythmic transcranial brain stimulation: level of control over oscillatory network activity. Front. Cell. Neurosci. 9. doi:10.3389/fncel.2015.00477.

Vieira, P.G., Krause, M.R., Pack, C.C., 2019. tACS entrains neural activity while somatosensory input is blocked. bioRxiv, 691022 doi:10.1101/691022.

Violante, I.R., Li, L.M., Carmichael, D.W., Lorenz, R., Leech, R., Hampshire, A., Rothwell, J.C., Sharp, D.J., 2017. Externally induced frontoparietal synchronization modulates network dynamics and enhances working memory performance. Elife 6, e22001. doi:10.7554/eLife.22001.

Vossen, A., Gross, J., Thut, G., 2015. Alpha power increase after transcranial alternating current stimulation at alpha frequency (α-tACS) reflects plastic changes rather than entrainment. Brain Stimulat. 8, 499–508. doi:10.1016/j.brs.2014.12.004.

Weinrich, C.A., Brittain, J.-.S., Nowak, M., Salimi-Khorshidi, R., Brown, P., Stagg, C.J., 2017. Modulation of Long-Range Connectivity Patterns via Frequency-Specific Stimulation of Human Cortex. Curr. Biol. 27, 3061–3068. doi:10.1016/j.cub.2017.08.075.

Weisz, N., Wühle, A., Monittola, G., Demarchi, G., Frey, J., Popov, T., Braun, C., 2014. Prestimulus oscillatory power and connectivity patterns predispose conscious somatosensory perception. Proc. Natl. Acad. Sci. 111, E417–E425. doi:10.1073/pnas.1317267111.

Wittenberg, M.A., Baumgarten, T.J., Schnitzler, A., Lange, J., 2018. U-shaped relation between prestimulus alpha-band and poststimulus gamma-band power in temporal tactile perception in the human somatosensory cortex. J. Cogn. Neurosci. 30, 552–564. doi:10.1162/jocn_a_01219.

Wöstmann, M., Herrmann, B., Maess, B., Obleser, J., 2016. Spatiotemporal dynamics of auditory attention synchronize with speech. Proc. Natl. Acad. Sci., 201523357 doi:10.1073/pnas.1523357113.

Wöstmann, M., Lim, S.-.J., Obleser, J., 2017. The human neural alpha response to speech is a proxy of attentional control. Cereb. Cortex 27, 3307–3317. doi:10.1093/cercor/bhx074.

Yaple, Z., Martinez-Saito, M., Awasthi, B., Feurra, M., Shestakova, A., Klucharev, V., 2017. Transcranial alternating current stimulation modulates risky decision making in a frequency-controlled experiment. eNeuro 4. doi:10.1523/ENEURO.0136-17.2017.

Zaehle, T., Rach, S., Herrmann, C.S., 2010. Transcranial alternating current stimulation enhances individual alpha activity in human EEG. PLoS ONE 5, e13766. doi:10.1371/journal.pone.0013766.

Zrenner, C., Desideri, D., Belardinelli, P., Ziemann, U., 2018. Real-time EEG-defined excitability states determine efficacy of TMS-induced plasticity in human motor cortex. Brain Stimulat. 11, 374–389. doi:10.1016/j.brs.2017.11.016.

Zumer, J.M., Scheeringa, R., Schoffelen, J.-.M., Norris, D.G., Jensen, O., 2014. Occipital alpha activity during stimulus processing gates the information flow to object-selective cortex. PLoS Biol. 12, e1001965. doi:10.1371/journal.pbio.1001965.

Zuo, X.-.N., Ehmke, R., Mennes, M., Imperati, D., Castellanos, F.X., Sporns, O., Milham, M.P., 2012. Network centrality in the human functional connectome. Cereb. Cortex 22, 1862–1875. doi:10.1093/cercor/bhr269.